available at www.sciencedirect.com

ScienceDirect

journal homepage: www.elsevier.com/locate/biochempharm

Antagonist-radioligand binding to D_{2L}-receptors in intact cells

Ann Packeu *, *Jean-Paul De Backer, Isabelle Van Liefde, Patrick M.L. Vanderheyden, Georges Vauquelin*

Free University of Brussels (VUB), Department of Molecular and Biochemical Pharmacology, Institute for Molecular Biology and Biotechnology, Pleinlaan 2, B-1050 Brussels, Belgium

ARTICLE INFO

Article history:
Received 19 November 2007
Accepted 6 March 2008

Keywords:
Dopamine receptor
Radioligand binding
Intact cells
Raclopride
Spiperone

ABSTRACT

D_2-dopamine receptors mediate most of the physiological actions of dopamine and are important recognition sites for antipsychotic drugs. Earlier binding studies were predominantly done with broken cell preparations with the tritiated D_2-receptor antagonists [^{3}H]-raclopride, a hydrophilic benzamide, and [^{3}H]-spiperone, a highly hydrophobic butyrophenone. Here we compared [^{3}H]-raclopride and [^{3}H]-spiperone binding properties in intact Chinese Hamster Ovary cells stably expressing recombinant human D_{2L}-receptors. Specific binding of both radioligands occurred to a comparable number of sites. In contrast to the rapid dissociation of [^{3}H]-raclopride in both medium only and in the presence of an excess of unlabelled ligand [^{3}H]-spiperone dissociation was only observed in the latter condition, and it was still slower than in broken cell preparations. However, this could not explain the pronounced difference in the potency of some unlabelled ligands to compete with both radioligands. To integrate these new findings, a model is proposed in which raclopride approaches the receptor from the aqueous phase, while spiperone approaches the receptor by lateral diffusion within the membrane.

1. Introduction

Dopamine receptors belong to the large family of G-protein-coupled receptor (GPCR) proteins that possess seven transmembrane alpha helices and are responsible for the transduction of a wide variety of signals across the cell membrane [1]. Dopamine receptors have been divided into D_1-like receptors (comprising D_1- and D_5-receptors), which stimulate adenylyl cyclase enzyme activity and cAMP production, and D_2-like receptors (comprising D_2-, D_3- and D_4-receptors), which suppress cAMP production [2,3]. D_2-receptors mediate some of the important physiological actions of dopamine, such as control of movement and prolactin secretion [4]. They exist as two alternatively spliced transcripts: the D_{2S} isoform and the D_{2L} isoform, with an extra 29 amino acid sequence in the third intracellular loop [5]. *In vivo* studies indicate that the D_{2L}-receptors are located postsynaptically, and that D_{2S}-receptors act as presynaptic inhibitory autoreceptors [6–8]. Both transcripts can couple to different G-proteins [9–11] and, although they display similar affinity for most agonists and antagonists, some pharmacological differences have been noted [12].

Antipsychotics with D_2-receptor antagonist properties are routinely administered to patients suffering from schizophrenia to attenuate their psychotic phases [13,14]. Those of

* *Corresponding author*. Tel.: +32 2 6291946; fax: +32 2 6291358.
E-mail address: apackeu@vub.ac.be (A. Packeu).

Abbreviations: CHO-K1, Chinese Hamster Ovary cells; CHO-AEQ, Chinese Hamster Ovary cells stably transfected with the cDNA for apo-aquorin of *Aquoria victoria*, as well as the GTP-binding protein $G_{\alpha 16}$; CHO-D_{2L}, CHO-AEQ cells stably transfected with the cDNA of the human D2DR (transcript variant 1).

0006-2952/$ – see front matter
doi:10.1016/j.bcp.2008.03.001

the first generation were characterised by their high potency and long-lasting D_2-receptor blockade [15]. However, this latter property has been held responsible for their predisposition for producing extrapyramidal side effects, due to the refractoriness of the occupied D_2-receptors in the striatum in responding to fast fluctuations in local dopamine concentration. By the same logic, the better tolerability of the novel generation of ''atypical'' antipsychotics has been attributed to their swifter dissociation from D_2-receptors, so that those in the striatum remain responsive to peaks in the dopamine concentration [16]. The clinical findings with antipsychotics clearly illustrate that receptor binding kinetics may influence the utility of a therapeutic drug [17,18]. In this respect, Copeland et al. [19] recently recommended that candidate drugs should not only be screened for their affinity but also for their residence time at their target receptor.

D_2-receptor radioligand binding studies are often performed with the tritiated antagonists [^{3}H]-raclopride and [^{3}H]-spiperone. While raclopride is a benzamide and hydrophilic, spiperone is a butyrophenone and highly hydrophobic [20]. Based on the observation that CB_1 cannabinoid receptor ligands avidly incorporate into lipid bilayers because of their hydrophobicity [21], the possibility arises that the difference in hydrophobicity between raclopride and spiperone impacts their interaction with the D_2-receptor. In line with this presumption, differences in the amount of high affinity sites for [^{3}H]-raclopride and [^{3}H]-spiperone have indeed been reported in many studies [22–25], although not in all [26,27]. Moreover, Hall et al. [28] found that [^{3}H]-raclopride bound to more sites in rat striatal membranes when sodium ions were present while [^{3}H]-spiperone binding was not affected by this cation.

The vast majority of previously published D_2-receptor binding studies have been carried out on plasma membranes and/or cell homogenates. Despite the predominance of this experimental approach, it is clear that membrane receptors and membrane-associated proteins generally lose part of their natural environment when cells have been disrupted. Typically, differences in ionic composition and redox potential between the sides of the plasma membrane, as well as the organising role of the cytoskeleton, are only present in intact cells. In addition, receptors which are normally occluded, due to their presence in intracellular elements like the endoplasmic reticulum, Golgi apparatus and different types of vesicles, may become exposed to the radioligands when cells are disrupted. Such considerations could explain why certain antagonists display different receptor binding characteristics in experiments using intact cells instead of membrane preparations thereof [29,30].

These considerations prompted us to compare [^{3}H]-raclopride and [^{3}H]-spiperone D_{2L}-receptor binding characteristics in intact cells. Recombinant cells (i.e., CHO-D_{2L} cells, CHO cells stably expressing the human dopamine D_{2L}-receptor) were developed for this purpose. This allowed the use of the untransfected CHO cells in control experiments dealing with receptor-independent phenomena. While [^{3}H]-raclopride dissociated swiftly from the D_2-receptor [^{3}H]-spiperone dissociation was extremely slow, especially in the absence of an excess of unlabelled ligand. To explain these observations, we propose a model in which spiperone approaches the receptor by lateral diffusion within the membrane, while the hydrophilic antagonist raclopride behaves more classically by diffusing within the aqueous phase.

2. Materials and methods

2.1. Materials

[^{3}H]-raclopride (60–63 Ci/mmol) and [^{3}H]-spiperone (79–113 Ci/mmol) were purchased from PerkinElmer (Boston, MA, U.S.A.) and Amersham (Buckinghamshire, U.K.), respectively. Clozapine, haloperidol, raclopride and spiperone were purchased from Tocris (Avonmouth, U.K.) and (±)-butaclamol from Sigma–Aldrich (St. Louis, MO, U.S.A.).

2.2. Cell culture and stable transfection

Chinese Hamster Ovary cells (CHO-K1) that were stably transfected with the cDNA for apo-aquorin of *Aquoria victoria* and with the GTP-binding protein $G_{\alpha 16}$ both of which were kindly donated by Dr. M. Detheux (Euroscreen s.a., Gosselies, Belgium). These CHO-AEQ cells were cultured in 75 cm^2 flasks using Dulbecco's Modified Essential Medium (DMEM) supplemented with 2 mM L-glutamine, 2% of a stock solution containing 5000 IU ml^{-1} penicillin and 5000 μg ml^{-1} streptomycin (Life Technologies, Merelbeke, Belgium), and 10% fetal bovine serum (Life Technologies, Merelbeke, Belgium). The cells were grown in 5% CO_2 at 37 °C. The pcDNA3.1 expression vector containing the entire coding region of the human D2DR (transcript variant 1) was obtained from UMR cDNA Resource Center (Rolla, MO, U.S.A.) and was transfected into CHO-AEQ cells using lipofectamine (Life Technologies, Merelbeke, Belgium) according to the manufacturer's instructions. Seventy-two hours after transfection the culture medium (see above) was replaced with medium containing 1 mg/ml geneticin (Life Technologies, Merelbeke, Belgium). After approximately five passages, the resulting stably transfected cells (denoted as CHO-D_{2L} cells) were further grown in supplemented DMEM and used in the present studies.

2.3. Binding experiments

CHO-D_{2L} cells were plated in polystyrene Costar® Corning® Cellbind® Surface 24-well plates (Elscolab, Kruibeke, Belgium) and cultured until confluence. Before the experiment, the cells were washed three times with 500 μl per well of HEPES-DMEM (binding buffer) (Life Technologies, Merelbeke, Belgium) at room temperature, and left for 15 min at 37 °C in 400 μl binding buffer for each well. At the end of all experiments, the 24-well plates were placed on ice and washed three times with ice-cold phosphate buffered saline (PBS, containing 0.132 g l^{-1} $CaCl_2{\cdot}2H_2O$, 0.2 g l^{-1} KCl, 0.2 g l^{-1} KH_2PO_4, 0.1 g l^{-1} $MgCl_2{\cdot}6H_2O$, 8 g l^{-1} NaCl and 1.44 g l^{-1} $Na_2HPO_4{\cdot}2H_2O$). Cells were then solubilized by addition of 300 μl 1 M NaOH and 200 μl H_2O. After 60 min treatment at room temperature, solutes were transferred in scintillation vials. The radioactivity was counted for 3 min in a liquid scintillation counter after addition of 3 ml of scintillation liquid (Optiphase Hisafe, PerkinElmer; Boston, MA, U.S.A.).

2.3.1. [^{3}H]-raclopride binding

All incubations were carried out at 37 °C for 30 min, or for the indicated time periods, in a final assay volume of 500 μl binding buffer. Total and non-specific binding of the radioligand was determined in the absence or presence of 1 μM spiperone (final concentration). The incubations were carried out with [^{3}H]-raclopride at final concentrations ranging between 0.25 and 8 nM for the saturation binding assays and at 2 nM for all other experiments. For the competition binding assays, cells were preincubated with increasing concentrations of unlabelled ligands (for 30 min at 37 °C) and, after addition of 2 nM [^{3}H]-raclopride, further incubated for 30 min at 37 °C. Dissociation binding assays were performed by incubating the cells with 2 nM radioligand (30 min, 37 °C), followed by two HEPES-DMEM washes and subsequent exposure of the cells to 500 μl fresh medium (binding buffer with or without 0.2% bovine serum albumin (BSA) from Sigma–Aldrich (St. Louis, MO, U.S.A.)), either alone or with addition of an excess of unlabelled raclopride (1 μM) or spiperone (1 μM) for the times indicated.

The apparent dissociation rate constants ($k_{-1(I)}$) of unlabelled antagonists were estimated based on their ability to delay the association of [^{3}H]-raclopride as described earlier [31]. In short, CHO-D_{2L} cells were preincubated for 30 min at 37 °C with 500 μl binding buffer containing unlabelled raclopride or spiperone. Cells were washed twice with binding buffer and incubated with 2 nM [^{3}H]-raclopride for increasing periods of time. Based on such experiments the $k_{-1(I)}$ values of unlabelled antagonists were calculated by computer-assisted iteration assuming a competitive interaction with [^{3}H]-raclopride, and that all antagonist–receptor interactions proceed according to a one-site bimolecular reaction obeying the mass action law. The $k_{-1(I)}$ values were adjusted until the computed [^{3}H]-raclopride binding versus time plots yielded the same apparent first-order rate constant as the experimental values.

2.3.2. [^{3}H]-spiperone binding

All incubations are carried out at 37 °C for 30 min, or for the indicated time periods, in a final assay volume of 500 μl BSA binding buffer (binding buffer with 0.2% BSA). Total and non-specific binding of the radioligand was determined in the absence or presence of 0.3 μM unlabelled (±)-butaclamol (final concentration). The incubations were carried out with [^{3}H]-spiperone at final concentrations ranging between 0.25 and 8 nM for the saturation binding assays and at 1 nM for all other experiments. For the competition binding assays the cells were preincubated at 37 °C for 30 min in 500 μl/well with increasing concentrations of unlabelled ligands. Subsequently 1 nM [^{3}H]-spiperone was added and cells were incubated at 37 °C for 30 min. Dissociation assays were performed by incubating the cells with 1 nM radioligand in 500 μl BSA binding buffer (30 min, 37 °C) followed by washing the cells twice with binding buffer, addition of 500 μl BSA binding buffer with or without 10 μM (±)-butaclamol and further incubation for the times indicated. For the experiments in Figs. 8–10 [^{3}H]-spiperone incubation was followed by two intermediary wash steps with binding buffer at 37 °C, and further incubation for 10 min at 37 °C with 500 μl BSA binding buffer.

2.4. Simulations

The computer-assisted simulations in Table 3 were performed as previously described [32] to generate antagonist IC_{50} values under the same conditions as those used in the competition binding studies shown in Figs. 3 and 10. All antagonist–receptor interactions were assumed to be reversible bimolecular interactions. The association (k_1) and dissociation (k_{-1}) rate constants of the radioligands were from the kinetic studies shown in Figs. 1, 4, 7 and 8 (k_{-1} values were from experiments in the presence of an excess of unlabelled ligand; k_1 values were calculated by the following equation: $k_1 = (k_{obs} - k_{-1})/[L]$, where k_{obs} is the experimental pseudo-first-order association rate constant and [L] the radioligand concentration). These kinetic constants were assumed to be the same for the unlabelled and labelled forms of the same antagonist. Simulated data rely on integrating the outcomes of the differential equations (yielding changes in the percentage of free receptors and in the different antagonist- and radioligand-bound forms of the receptor over very small time periods) over time for periods corresponding to 30 min for the preincubation with different concentrations (1/2 log intervals between 0.01 and 3000 nM) of unlabelled antagonist only, and for time periods corresponding to 30 min for the ensuing incubation with unlabelled plus labelled antagonist combinations (2 nM [^{3}H]-raclopride or 1 nM [^{3}H]-spiperone (i.e., the same as in the competition experiments shown in Figs. 3 and 10). The simulated radioligand binding data versus the log (free antagonist concentration) plots were sigmoidal. As for the experimental data, the simulated competition binding plots were analysed by GraphPad Prism™ (San Diego, CA, U.S.A.) to yield the IC_{50} values of the unlabelled ligands.

2.5. Data analysis

All experimental values are shown as the mean ± S.E.M. of at least three independent experiments (each performed in duplicate or triplicate). The half maximal inhibitory concentration values (IC_{50}) from competition binding experiments, the K_D and the B_{max} values from saturation binding curves and kinetic constants from time curves were calculated by non-regression analysis by GraphPad Prism™ based on a one-site bimolecular reaction obeying the Law of Mass Action. For curve fitting in the competition binding experiments, a one-site model was used with free-floating 100% and 0% equal to non-specific binding (i.e., in presence of 1 μM spiperone or 0.3 μM (±)-butaclamol).

3. Results

3.1. [^{3}H]-raclopride binding

Incubation of CHO-D_{2L} cells at 37 °C with 2 nM [^{3}H]-raclopride resulted in a time-dependent increase in specific binding that reached steady-state value in approximately 15 min. The corresponding pseudo-first-order rate constant for association (k_{obs}) was 0.23 ± 0.04 min^{-1} (Fig. 1). Non-specific binding of this radioligand was below 5% of total binding and no specific binding could be detected when the same experiment was

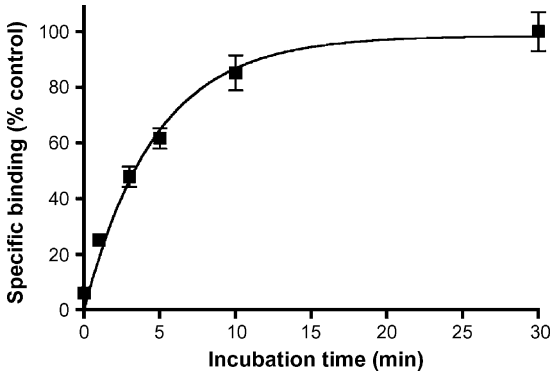

Fig. 1 – [^{3}H]-raclopride association binding to human D_{2L}-dopamine receptors in intact CHO-D_{2L} cells. Cells were incubated at 37 °C with 2 nM [^{3}H]-raclopride for different periods of time. Specific binding is expressed as percentage of steady-state specific binding after 30 min, N = 3.

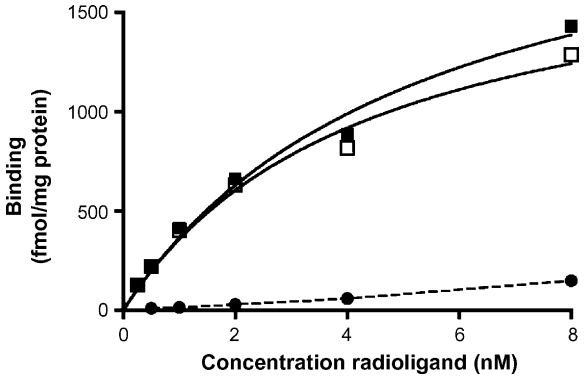

Fig. 2 – Saturation binding of [^{3}H]-raclopride. Intact CHO-D_{2L} cells were incubated for 30 min at 37 °C with increasing concentrations of [^{3}H]-raclopride. Data refer to the total binding (■), non-specific binding in the presence of 1 μM unlabelled spiperone (●) and specific binding calculated by subtracting non-specific from total binding (□). Data are expressed as fmol/mg protein. Data are from a representative experiment, N = 6.

performed on native CHO-AEQ cells. Specific binding of [^{3}H]-raclopride to intact CHO-D_{2L} cells was saturable (Fig. 2). Binding increased with the free radioligand concentration following a hyperbolic function yielding a total amount of sites (B_{max}) of 1,239 ± 202 fmol/mg protein and an equilibrium dissociation constant (K_D) of 5.10 ± 0.55 nM.

Unlabelled D_2-receptor antagonists caused a full and concentration-dependent inhibition of the specific binding of 2 nM [^{3}H]-raclopride (Fig. 3). The order of potency of these antagonists was spiperone > haloperidol > butaclamol > raclopride ≫ clozapine. The corresponding pK_i values are shown in Table 1.

For dissociation experiments, cells were preincubated for 30 min at 37 °C with 2 nM [^{3}H]-raclopride and rapidly washed. Dissociation at 37 °C was then monitored for different periods of time under two different conditions. First, cells were further

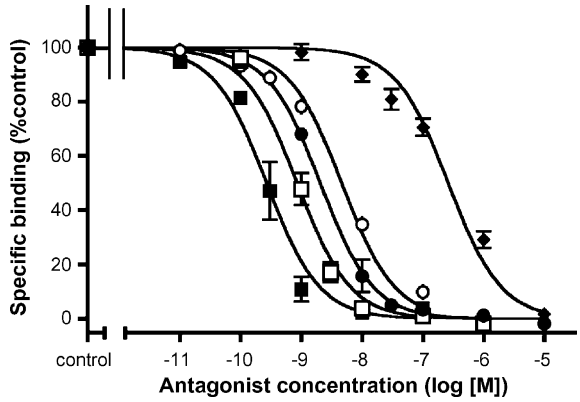

Fig. 3 – Competition between unlabelled D_2-receptor antagonists and [^{3}H]-raclopride. Intact CHO-D_{2L} cells were preincubated for 30 min at 37 °C in the absence (control binding) or presence of increasing concentrations of spiperone (■), haloperidol (□), (±)-butaclamol (●), raclopride (○) and clozapine (◆) followed by a 30 min incubation with 2 nM of [^{3}H]-raclopride. Specific binding is expressed as percentage of control binding. The corresponding pK_i values of the unlabelled antagonists are given in Table 1, N = 3–5.

incubated with fresh medium containing 1 μM spiperone or 1 μM raclopride. Under this condition [^{3}H]-raclopride binding decreased exponentially and the majority of specific binding sites were freed by the end of the experiment, i.e., after 60 min (Fig. 4). The corresponding dissociation rate constants (k_{-1}) were 0.12 ± 0.01 min^{-1} ($t_{1/2}$ = 5.75 min) in the presence of 1 μM spiperone and 0.15 ± 0.04 min^{-1} ($t_{1/2}$ = 4.60 min) in the presence of 1 μM raclopride. For the second procedure, the cells were further incubated in fresh medium alone. Under this condition, dissociation of [^{3}H]-raclopride only took place from approximately 80% of the sites. However, the dissociation could still be fit to an exponential function and the k_{-1} of 0.11 ± 0.01 min^{-1} ($t_{1/2}$ = 6.27 min) was similar to the values obtained in the first procedure. Omission of 0.2% BSA in the binding buffer did not affect the radioligand dissociation in either case (data not shown).

Table 1 – Antagonist pK_i-values for the D_{2L}-receptors in intact CHO-D_{2L} cells

Antagonist	Calculated competition binding data radioligand	
	[^{3}H]-raclopride	[^{3}H]-spiperone
Butaclamol	8.96 ± 0.06	9.17 ± 0.03
Clozapine	6.88 ± 0.11	>6
Haloperidol	9.35 ± 0.08	8.86 ± 0.27
Raclopride	8.62 ± 0.04	7.32 ± 0.17
Spiperone	9.84 ± 0.10	10.16 ± 0.14

pK_i values are calculated using the Cheng and Prusoff equation from the IC_{50} and kinetic K_D ([^{3}H]-raclopride = 2.20 nM and [^{3}H]-spiperone = 0.11 nM) values. Data are the mean ± S.E.M. of 3–5 independent experiments illustrated in Figs. 3 and 10.

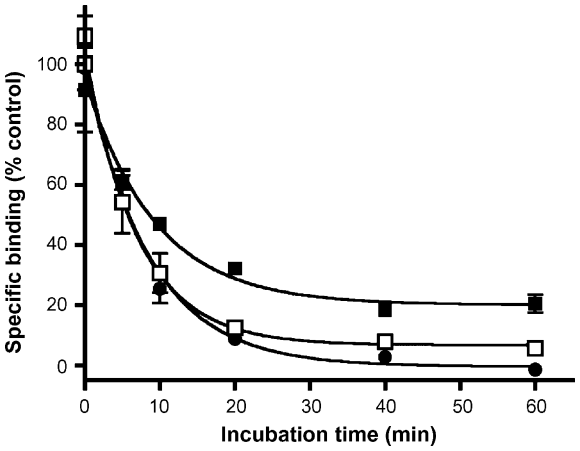

Fig. 4 – Dissociation of [^{3}H]-raclopride from human D_{2L}-dopamine receptors in intact CHO-D_{2L} cells. Cells were incubated for 30 min at 37 °C with 2 nM [^{3}H]-raclopride and its dissociation was initiated by washing of the cells and replacement with fresh medium (binding buffer with 0.2% BSA) either alone (■) or containing 1 μM unlabelled raclopride (□) or 1 μM unlabelled spiperone (●). Binding is expressed as percentage of specific binding immediately after washing, N = 3.

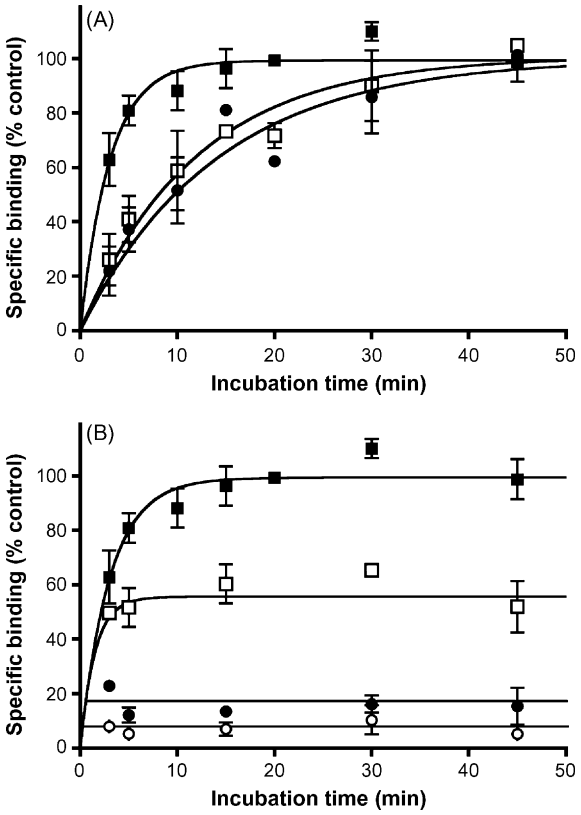

Fig. 5 – Effect of raclopride and spiperone preincubation on the apparent association rate of [^{3}H]-raclopride. Intact CHO-D_{2L} cells were incubated for 30 min at 37 °C with 30 nM (□) or 100 nM (●) raclopride (panel A) or with 0.3 nM (□), 1 nM (●) or 3 nM (○) spiperone (panel B), washed and finally incubated at 37 °C with 2 nM [^{3}H]-raclopride for different periods of time. Specific binding is expressed as percentage of control binding (■), i.e., binding after 30 min radioligand incubation in the absence of antagonist pretreatment, N = 3–7.

The dissociation rate of unlabelled raclopride and spiperone were also estimated indirectly. In these experiments, cells were preincubated with a high (near receptor-saturating) concentration of unlabelled ligand, washed and finally incubated with 2 nM [^{3}H]-raclopride for increasing time periods. Preincubation with 30 and 100 nM raclopride did not affect the maximal extent of the subsequent [^{3}H]-raclopride binding but it effectively delayed the association of this radioligand (Fig. 5A); the k_{obs} increased from 0.23 to 0.14 min^{-1} or 0.13 min^{-1} after preincubation with 30 and 100 nM raclopride, respectively. Assuming that the dissociation of the pre-formed raclopride D_{2L}-receptor complexes is necessary for [^{3}H]-raclopride binding to take place, the dissociation rate of raclopride could be calculated from the delay in [^{3}H]-raclopride association [31]. The calculated k_{-1}-value (0.16 min^{-1}) was comparable to the value obtained from the direct [^{3}H]-raclopride dissociation experiments (0.12–0.15 min^{-1}, Fig. 4). On the other hand, following preincubation with a high concentration of spiperone, almost no recovery of [^{3}H]-raclopride binding was found to take place (Fig. 5B). When this experiment was repeated with a lower spiperone concentration (i.e., at which only half of the receptors were occupied), recovery of [^{3}H]-raclopride binding proceeded with the same k_{app} as for untreated cells, but the number of labelled sites was only half. These experiments suggest that spiperone dissociates so slowly that the receptor proteins involved remain unavailable to [^{3}H]-raclopride for at least 60 min.

3.2. [^{3}H]-spiperone binding

Binding of 1 nM [^{3}H]-spiperone to CHO-D_{2L} cells was decreased in a concentration-dependent fashion by (±)-butaclamol, as well as by other D_2-receptor antagonists (data not shown). Compared to the nearly full inhibition (≥95%) in similar experiments with [^{3}H]-raclopride, only about 50% of the total [^{3}H]-spiperone binding could be inhibited by the presence of high concentrations of (±)-butaclamol (Fig. 6). In contrast, binding of [^{3}H]-spiperone to the non-transfected CHO-AEQ cells showed little sensitivity to (±)-butaclamol with a level that closely matched that of the (±)-butaclamol-resistant [^{3}H]-spiperone binding in CHO-D_{2L} cells. Based on these data, only (±)-butaclamol-sensitive [^{3}H]-spiperone binding to the CHO-D_{2L} cells was considered to represent "specific" D_2-receptor binding.

Subsequently, the dissociation kinetics of (±)-butaclamol-sensitive and insensitive [^{3}H]-spiperone binding were investigated. These experiments confirmed the slow-dissociating binding of this radioligand to D_2-receptors, and provided the rationale for a procedure to dramatically reduce non-specific binding without affecting specific binding in association, saturation and competition experiments.

In the experiments shown in Fig. 7A–C, cells were incubated for 30 min with 1 nM [^{3}H]-spiperone, washed and further

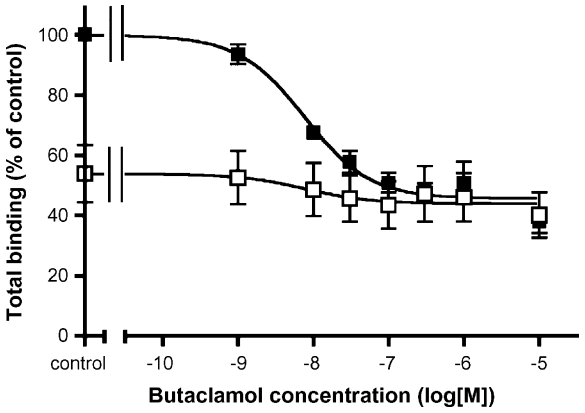

Fig. 6 – Effect of (±)-butaclamol on total [^{3}H]-spiperone binding to CHO-D_{2L} cells (■) and CHO-AEQ cells (□). Intact cells were preincubated for 30 min at 37 °C with increasing concentrations of (±)-butaclamol and then further incubated for 30 min with 1 nM of [^{3}H]-spiperone. Binding is expressed as percentage of control binding (i.e., binding in the absence of (±)-butaclamol) to the same amount of CHO-D_{2L} cells, $N = 3$.

incubated for up to 120 min with fresh buffer alone or buffer containing either 2 nM unlabelled raclopride or 10 μM unlabelled (±)-butaclamol. Of note was a lack of dissociation of specific [^{3}H]-spiperone binding from CHO-D_{2L} cells in fresh medium or in the presence of a low concentration of raclopride (2 nM) (Fig. 7C). In the presence of 10 μM (±)-butaclamol, specific [^{3}H]-spiperone binding decreased mono-exponentially with a k_{-1} of 0.0069 min^{-1} ($t_{1/2}$ = 100 min) (Fig. 7C). After 120 min of wash-out, specific [^{3}H]-spiperone binding decreased to an extent comparable to that observed in the presence of a large excess of raclopride or other antagonists (Table 2). Additionally, non-specifically bound [^{3}H]-spiperone dissociated rapidly from the CHO-D_{2L} cells, either in buffer alone (Fig. 7A) or in the presence of a large excess (±)-butaclamol (Fig. 7B). Dissociation of total [^{3}H]-spiperone binding from non-transfected CHO-AEQ cells was equally rapid (Fig. 7D). The biphasic dissociation of total [^{3}H]-spiperone binding in the presence of (±)-butaclamol (Fig. 7B) resulted from the rapid dissociation of the non-specific binding along with the slower dissociation of the specific binding.

To reduce the extent of non-specific [^{3}H]-spiperone binding without affecting its specific binding, further experiments were terminated by including a brief incubation of the cells with BSA binding buffer (10 min at 37 °C) at the end of the wash steps. Under these conditions, incubation of CHO-D_{2L} cells at 37 °C with 1 nM [^{3}H]-spiperone resulted in a time-dependent increase in specific binding reaching a steady-state value after about 30 min. The corresponding pseudo-first-order rate constant for association (k_{obs}) was 0.07 ± 0.01 min^{-1} (Fig. 8). Specific binding of [^{3}H]-spiperone was saturable (Fig. 9) involving a single class of sites with an apparent equilibrium dissociation constant (K_d) of 0.94 ± 0.28 nM. The B_{max} value (1.119 ± 88 fmol/mg protein) of [^{3}H]-spiperone was not significantly different from the value obtained with [^{3}H]-raclopride ($P > 0.05$). The order of potencies of unlabelled D_2-receptor antagonists in competing with specific [^{3}H]-spiperone binding was spiperone > butaclamol ≅ haloperidol > raclopride ≫ clozapine (Fig. 10). The corresponding apparent pK_i values are given in Table 1. Only the three most potent antagonists were able to provoke full inhibition at the concentrations used.

4. Discussion

This present findings provide new insights on the D_{2L}-dopamine receptor binding properties of the antagonists [^{3}H]-raclopride and [^{3}H]-spiperone to intact cells, i.e., recombinant CHO cells stably expressing the gene encoding for the D_{2L}-receptor. The saturation, competition and kinetic data support a single class of sites for both radioligands. However, the experiments revealed two interesting differences between the radioligands. [^{3}H]-spiperone dissociated much slower than [^{3}H]-raclopride, although this could not explain the ratio between raclopride and spiperone in competition binding studies with both radioligands. It is proposed therefore that both radioligands bind to the same receptor protein or complex, but that they undergo different modes of transport to and from the receptor.

Specific binding of the benzamide [^{3}H]-raclopride and butyrophenone [^{3}H]-spiperone can readily be observed in the recombinant CHO-D_{2L} cells, but not in untransfected CHO-AEQ cells. For specific binding, the association and dissociation curves were mono-exponential (Figs. 1, 4, 7 and 8) for both radioligands and the level of binding (Figs. 2 and 9) increased with free concentration according to a hyperbolic function. These data are in agreement with a simple bimolecular ligand–receptor interaction. Saturation binding experiments further indicated that the specific binding of these radioligands involves the same number of sites. Together, these findings suggest that both ligands bind to a single class of sites present on the same population of D_{2L}-receptor molecules (or molecular complexes). While the present study on intact cells was performed at 37 °C, similar B_{max} values were found by Itokawa et al. [33] when comparing [^{3}H]-spiperone and [^{3}H]-raclopride binding to similar recombinant CHO-D_{2L} cells at 4 °C, i.e., a temperature which is to low for receptor internalization to take place. This similarity was especially interesting in light of the contention that [^{3}H]-spiperone is lipophilic and able to bind intracellular as well as extracellular receptors, while [^{3}H]-raclopride (and related hydrophilic ligands) only binds to receptors at the cell surface [33–35]. Indeed, this similarity provides a strong indication that, in the present study, specific binding of [^{3}H]-spiperone only takes place to D_{2L}-receptors that are present at the extracellular face of the cell membrane. This was also indirectly supported by studies showing that the internalization of D_2-receptors was triggered by dopamine but not by D_2-receptor antagonists [33], and that the amount of intracellular D_2-receptors was minimal in the absence of dopamine [36]. That binding of [^{3}H]-spiperone to intracellular D_{2L}-receptors might be reflected as non-specific binding is unlikely since, in the present study, it was similar to the total (and non-displaceable) [^{3}H]-spiperone binding in the parent CHO-AEQ cells.

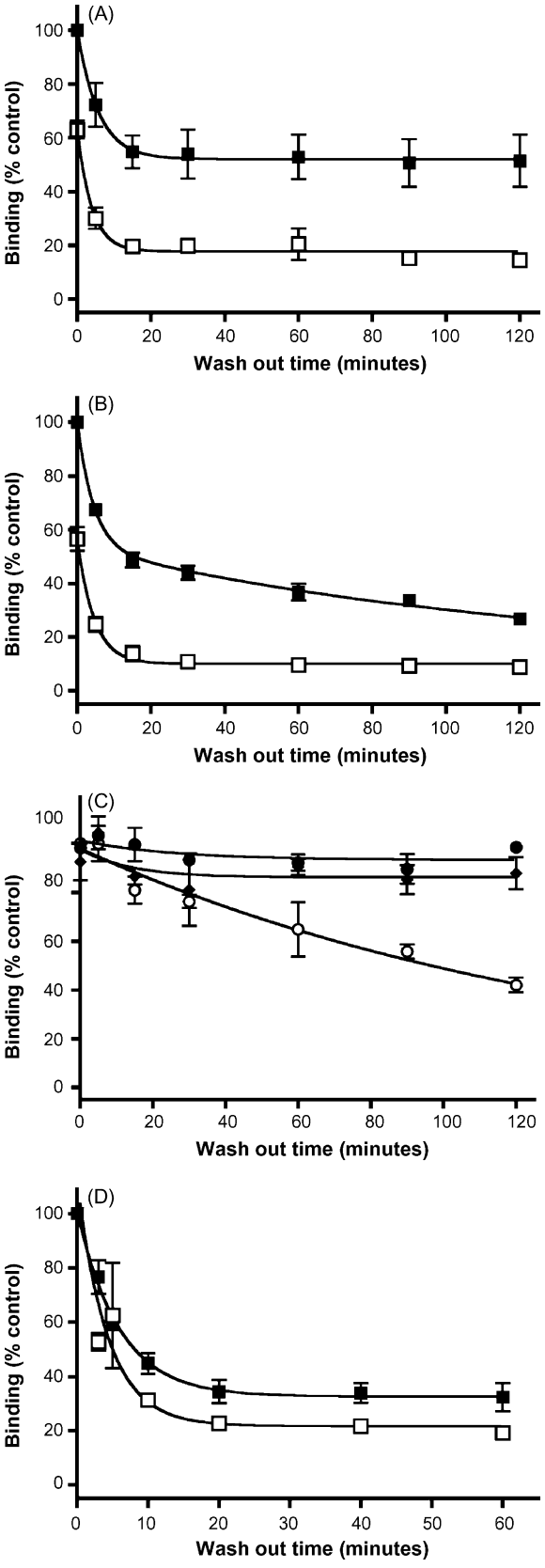

Fig. 7 – Dissociation of [^{3}H]-spiperone from intact cells. Cells were incubated for 30 min at 37 °C with 1 nM [^{3}H]-spiperone and its dissociation was initiated by washing of the cells and replacement with fresh medium (binding buffer with 0.2% BSA) with or without additions of unlabelled ligand. Panel (A) CHO-D_{2L} cells; dissociation in medium only: total binding (■) and non-specific binding (□) of [^{3}H]-spiperone are presented as percentage of total binding immediately after washing. Panel (B) CHO-D_{2L} cells; dissociation in medium containing 10 μM unlabelled (±)-butaclamol: total binding (■) and non-specific binding (□) of [^{3}H]-spiperone. Panel (C) CHO-D_{2L} cells; dissociation of specific [^{3}H]-spiperone binding (presented as percentage of specific binding immediately after washing) in medium either alone (◆), calculated from data shown in panel (A) or containing 10 μM unlabelled (±)-butaclamol ((○), calculated from data shown in panel (B)) or 2 nM unlabelled raclopride (●). Panel (D) non-transfected CHO-AEQ cells; dissociation in medium only: total binding (■) and non-specific binding (□) of [^{3}H]-spiperone.

Table 2 – Dissociation of [^{3}H]-spiperone in presence of 10 μM of different unlabelled ligands

Antagonist in wash-out buffer	Dissociated [^{3}H]-spiperone after 120 min wash-out
Butaclamol	62 ± 4
Spiperone	61 ± 5
Raclopride	54 ± 8
Haloperidol	49 ± 2

Experiments were performed as in Fig. 7C: CHO-D_{2L} cells were incubated for 30 min at 37 °C with 1 nM [^{3}H]-spiperone, washed twice with binding buffer and incubated for 120 min with 500 μl BSA binding buffer containing 10 μM of the listed unlabelled antagonists. Values refer to the amount (±S.E.M., $N = 3$) of dissociated specific binding.

Studies with cell membrane preparations yield distinct D_2-receptor binding capacities when comparing radiolabelled benzamides and butyrophenones [24,28,37,38]. However, this could reflect the ionic composition of the incubation medium. Indeed, in membrane preparations from different sources, including brain tissues expressing endogenous D_2-receptors and Sf9 or CHO cells expressing recombinant D_2-receptors [^{3}H]-raclopride binding was dependent on the presence of sodium ions, whereas [^{3}H]-spiperone and *N*-[^{3}H]-methylspiperone binding was not [28,37,38]. When the experiments were done in the presence of a sufficient concentration of sodium chloride, comparable radiolabelled benzamide and butyrophenone binding capacities were observed in some [27,28,37] but not all [24,38] membrane preparations. Additionally, benzamides and butyrophenones do not necessarily bind to the same state of the D_2-receptor. To explain the higher binding capacity of [^{3}H]-spiperone in membranes from several tissues (despite the presence of sodium chloride), butyrophenone binding was proposed to be restricted to the monomeric form of the receptor while benzamides were thought to bind to both the mono- and dimeric forms [24]. This suggests that the binding capacity of both types of ligands reflects the equilibrium between mono- and dimeric forms of the receptor in each preparation. In light of these considerations, and taking in account that intact cell binding studies are routinely performed in the presence of sodium chloride, the similar D_2-receptor binding capacities for [^{3}H]-raclopride and

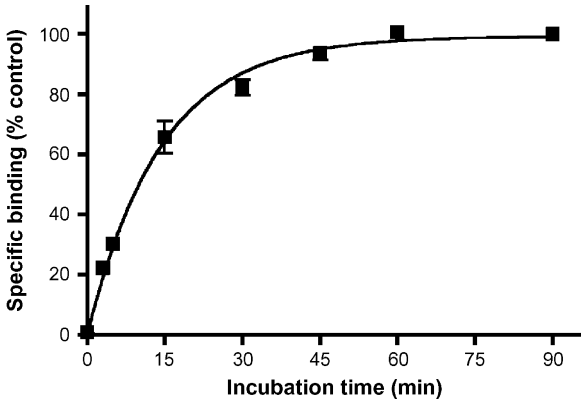

Fig. 8 – [^{3}H]-spiperone association binding to human D_{2L}-dopamine receptors in intact CHO-D_{2L} cells. Cells were incubated at 37 °C with 1 nM [^{3}H]-spiperone in BSA binding buffer for different periods of time. Specific binding is expressed as percentage of steady-state specific binding after 90 min, N = 3.

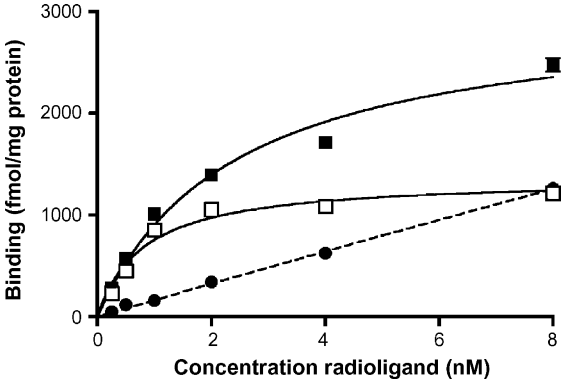

Fig. 9 – Saturation binding of [^{3}H]-spiperone. Intact CHO-D_{2L} cells were incubated for 30 min at 37 °C with increasing concentrations of [^{3}H]-spiperone. Data refer to the total binding (■), non-specific binding in the presence of 0.3 μM unlabelled (±)-butaclamol (●) and specific binding calculated by subtracting non-specific from total binding (□). Data are expressed as fmol/mg protein. Data are from a representative experiment, N = 6.

[^{3}H]-spiperone in intact CHO cells (present experiments and those of Itokawa et al. [33]) suggest that nearly all receptors present in these cells are monomers.

Because of the important implications of D_2-receptor dissociation kinetics in neuroleptic drug therapy, we focused on this issue to identify for a convenient method to determine the dissociation of antagonist–D_2-receptor complexes without the need for radiolabelled forms. Recently, we successfully applied this approach to monitor dissociation of non-peptide antagonists from AT_1 type angiotensin II receptors in a recombinant CHO cell line. This involved producing nearly complete receptor occupancy by unlabelled antagonist during a preincubation step, washing to remove free antagonist and, finally, following the recovery of receptor binding capacity/

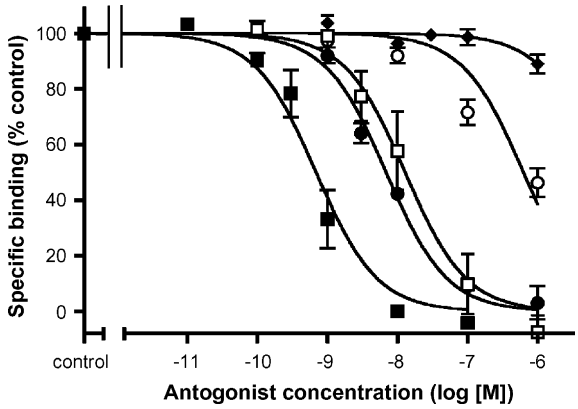

Fig. 10 – Competition between unlabelled D_2-receptor antagonists and [^{3}H]-spiperone. Intact CHO-D_{2L} cells were preincubated for 30 min at 37 °C in the absence (control binding) or presence of increasing concentrations of spiperone (■), haloperidol (□), (±)-butaclamol (●), raclopride (○) and clozapine (◆) followed by a 30 min incubation with 1 nM of [^{3}H]-spiperone. Binding is expressed as percentage of specific control binding. The corresponding pK_i values of the unlabelled antagonists are given in Table 1, N = 3–5.

functionality over time. The dissociation rate of the unlabelled antagonist could then be calculated based on: (1) the delayed association of subsequently added radioligand or (2) the time needed for receptor function to recover.

We successfully adapted the "delayed radioligand association" technique to determine the dissociation half-life of antagonist/D_2-receptor complexes in CHO-D_{2L} cells. [^{3}H]-raclopride was considered as the radioligand of choice because of its very low level of non-specific binding. The binding of this radioligand was also consistent with a single-site interaction since association and dissociation curves were mono-exponential (Figs. 1 and 4). Using this technique, the calculated dissociation half-life of unlabelled raclopride (4.3 min, Fig. 5A) was found to be similar to the value obtained by directly measuring the dissociation of [^{3}H]-raclopride (4.6–5.8 min, Fig. 4). These values were also in the same range as those obtained when studying dissociation of [^{3}H]-raclopride from D_2-receptors in cell membranes (4.0–6.4 min; [39,40]). On the other hand, preincubation of the CHO-D_{2L} cells with spiperone completely prevented the specific binding of the subsequently added [^{3}H]-raclopride for at least 60 min. Similarly, no further [^{3}H]-raclopride binding occurred after preincubation with submaximal concentrations of spiperone (Fig. 5B). This phenomenon was also observed at low concentrations of spiperone, i.e., when only some of the receptors were occupied.

A possible explanation for this finding is that, once formed, the spiperone/D_{2L}-receptor complexes dissociated sufficiently slowly that binding of [^{3}H]-raclopride was prevented for a long time period. Alternatively, spiperone may trigger or stabilise a particular raclopride-refractory conformation of the D_{2L}-receptor, that persists after spiperone has dissociated from the receptor. This second possibility is based on the "coupling

model'' of de Chaffoy de Courcelles [41], and the notion that GPCRs can adopt a multitude of conformations and that each ligand only stabilises a certain subset of these [42,43]. However, kinetic experiments in which the dissociation of [^{3}H]-spiperone was directly measured argue in favour of the first explanation. Indeed, as shown in Fig. 7C, no measurable dissociation of [^{3}H]-spiperone took place from specific binding sites in either fresh medium or in fresh medium containing 2 nM raclopride (i.e., the same condition as in the ''delayed [^{3}H]-raclopride association'' experiment sin Fig. 5B). This is in apparent conflict with spiperone being a reversible D_2-receptor–antagonist. However, this conclusion is based on experiments in membrane preparations where dissociation of [^{3}H]-spiperone was invariably initiated by adding a large excess of unlabelled ligand. When the same experimental protocol was applied to the intact CHO-D_{2L} cell system, specific binding of [^{3}H]-spiperone was decreased in a time-dependent manner (Fig. 7C). Dissociation occurred mono-exponentially with a half-life of 100 min. This was slower than seen in the studies on cell and tissue membrane preparations (half-life of ~12 min [44]). While this could be considered due to differences in the experimental conditions, e.g., buffer composition, it is also possible that an intact cellular environment plays a role in stabilizing the D_{2L}-receptor in a particular conformation.

Accelerated radioligand dissociation in the presence of an excess of unlabelled ligand has already been observed for many receptor types and there are currently two major explanations to explain this phenomenon [45]. The work by De Meyts et al. [46] on insulin receptors, indicates that this may reflect negative cooperativity and, more specifically in the case of GPCRs, the existence of negative allosteric interactions between different ligand binding sites at the same receptor or di/multimeric receptor complex [47–49]. According to this allosteric model, our dissociation data implies that the butyrophenone-binding site for [^{3}H]-spiperone is topologically distinct from that for butaclamol [50,51]. An alternative explanation is that radioligand dissociation is only correctly measured in the presence of unlabelled ligand due its ability to prevent interfering reassociation phenomena. It is suggested that the radioligand can effectively dissociate from its receptor in medium alone, but that, once dissociated, it can reassociate to the same receptor or receptors nearby which would reflect an apparent delay in the observed radioligand dissociation [52]. When present at high concentrations, unlabelled ligand molecules (such as butaclamol) should immediately occupy the receptors after dissociation of bound radioligand (such as [^{3}H]-spiperone) so that radioligand reassociation does not occur. It is only with these conditions that an accurate radioligand dissociation rate of the radioligand is recorded [53] since once released, the radioligand becomes evenly distributed through the wash medium [48,54]. However, as receptors are present on the cell membranes (and, hence, unevenly distributed), released radioligand molecules may accumulate in the receptor vicinity if their reassociation is faster than diffusion [55–58]. In this respect, recent simulations by Gopalakrishnan et al. [52] indicated that ligand reassociation is favoured when receptors are in close vicinity of each other, when clustered in lipid rafts and/or when the (radio)ligand undergoes non-specific adsorption to the cell surface. Biophysical considerations further suggest that adsorbed ligands preferentially undergo two-dimensional surface diffusion to the receptor (i.e., obeying reduction-of-dimensionality kinetic) [55,59]. In the case of certain amphiphilic AT_1 receptor and CB_1 cannabinoid receptor ligands, it was recently proposed that these penetrate the receptors sideways, i.e., via the interface between the membrane lipids and the receptor TM domains [21,51,60–62]. A similar mechanism may also be proposed for spiperone. Studies addressing the transfer of this ligand into membranes and liposomes formed from membrane lipids revealed that it partitions avidly from the aqueous medium into the lipid bilayer [20]. Control experiments with empty 24-well plates indicated that plastic binding represents only a minor part of the non-specific binding of [^{3}H]-spiperone in CHO cell-containing well plates (<1/3, data not shown). Moreover, equal amounts of non-specific binding were measured in CHO-D_{2L}- and non-transfected CHO-AEQ cell-containing wells and, in both cases it was rapid and reversible (Figs. 6 and 7). Taken together, these findings suggest that spiperone interacts with lipids at the cell surface. It is therefore conceivable that this antagonist penetrates the D_2-receptor via a ''sideways'' type mechanism after having undergone a lateral diffusion within the external leaflet of the membrane bilayer. In contrast, the hydrophilic benzamide-based antagonist, raclopride appears to approach the receptor via a classical mechanism; i.e., by diffusing within the aqueous solution to the receptor surface. Both modes of interaction are schematically represented in Fig. 11.

This model represents an intriguing working hypothesis, as it allows the existence of allosteric interactions between different classes of D_2-receptor antagonists as well as non-conventional binding kinetics. In this respect, both concepts (either alone or together) could offer a potential explanation for why the potency ratios between spiperone and other antagonists like raclopride and clozapine are markedly higher in competition binding studies with [^{3}H]-spiperone when compared to those with [^{3}H]-raclopride (Figs. 3 and 10 and

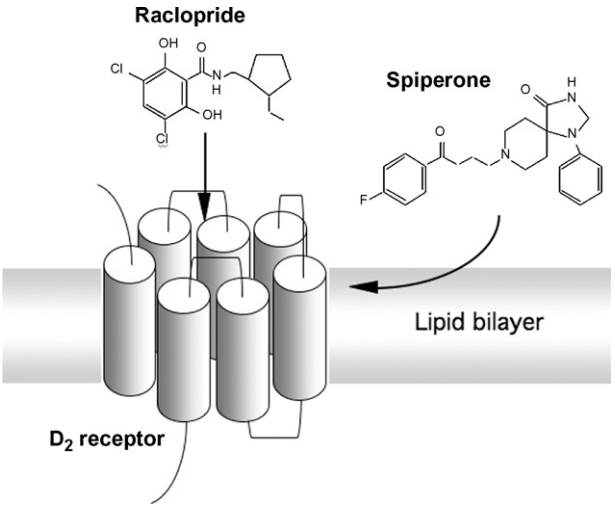

Fig. 11 – Proposed model wherein the hydrophilic raclopride approaches the receptor from the aqueous phase, while the hydrophobic spiperone approaches the receptor by lateral diffusion within the membrane.

Table 3 – Comparison between simulated and experimental IC_{50}-values of raclopride and spiperone

Radioligand	Antagonist	$I + R \Leftrightarrow^{k_1}_{k_{-1}} IR^*$, antagonist		IC_{50} (nM)	
		k_1 ($\times 10^{+7}$ M^{-1} min^{-1})	k_{-1} (min^{-1})	Simulations	Experimental
[^{3}H]-raclopride	Raclopride	5.5	1.2×10^{-1}	4.0	4.7
[^{3}H]-raclopride	Spiperone	6.3	6.9×10^{-3}	0.3	0.3
[^{3}H]-spiperone	Raclopride	5.5	1.2×10^{-1}	4.4	663.0
[^{3}H]-spiperone	Spiperone	6.3	6.9×10^{-3}	0.3	0.8

Computer-assisted simulations were performed as described under Section 2.

Table 1). This discrepancy did not occur in the simulated competition binding curves of those ligands (Table 3), if the simulations were performed using the classical equations based on the premise that each ligand interacts with the receptor according to the Law of Mass Action, that they are competitive with one another and, that the ligands and receptors are uniformly dispersed in solution [63]. Finally, it is of interest to note that the spiperone/raclopride potency ratios for the competition experiments with [^{3}H]-spiperone and [^{3}H]-raclopride in the present study on intact cells (692- and 17-fold, respectively) are similar to those found in competition binding studies with both radioligands on membrane preparations from recombinant D_2-receptor expressing cell lines (513- and 16-fold, respectively in [64,65]). Moreover, the ratio obtained with the binding studies with [^{3}H]-raclopride were also similar to that obtained when examining the inhibitory effect of spiperone and raclopride on constitutive D_2-receptor activity (measured with the [^{35}S]GTPγS binding technique) in membrane preparations (26-fold in [64]).

In conclusion, the major finding of the present work is that it compares the binding properties of two radioligands [^{3}H]-raclopride and [^{3}H]-spiperone, to D_2-dopamine receptors in intact cells rather than in membrane preparations thereof. This approach simplifies this comparison (i.e., both antagonists bind to a single class of sites present at the same receptor molecule or molecular complex), but raises issues regarding their dissociation kinetics and competition binding properties. To provide a potential explanation for these issues, a model is proposed in which the hydrophilic raclopride approaches the receptor from the aqueous phase while the hydrophobic spiperone relies instead on the lipid environment. We especially hope that this model will engender more interest in the important question on how to better clarify the interaction of hydrophobic ligands with their membrane-associated receptors.

Acknowledgments

We are most obliged to the 'Fonds voor Wetenschappelijk Onderzoek Vlaanderen' for their financial support. P.V. is holder of a 'Vrije Universiteit van Brussel' research fellowship.

REFERENCES

[1] Picetti R, Saiardi A, Abdel Samad T, Bozzi Y, Baik JH, Borrelli E. Dopamine D2 receptors in signal transduction and behavior. Crit Rev Neurobiol 1997;11:121–42.
[2] Kebabian JW, Calne DB. Multiple receptors for dopamine. Nature 1979;277:93–6.
[3] Stoof JC, Kebabian JW. Opposing roles for D-1 and D-2 dopamine receptors in efflux of cyclic AMP from rat neostriatum. Nature 1981;294:366–8.
[4] Velasco M, Luchsinger A. Dopamine: pharmacologic and therapeutic aspects. Am J Ther 1998;5:37–43.
[5] Dal Toso R, Sommer B, Ewert M, Herb A, Pritchett DB, Bach A, et al. The dopamine D2 receptor: two molecular forms generated by alternative splicing. EMBO J 1989;8:4025–34.
[6] Usiello A, Baik JH, Rouge-Pont F, Picetti R, Dierich A, LeMeur M, et al. Distinct functions of the two isoforms of dopamine D2 receptors. Nature 2000;408:199–203.
[7] Wang Y, Xu R, Sasaoka T, Tonegawa S, Kung MP, Sankoorikal EB. Dopamine D2 long receptor-deficient mice display alterations in striatum-dependent functions. J Neurosci 2000;20:8305–14.
[8] Lindgren N, Usiello A, Goiny M, Haycock J, Erbs E, Greengard P, et al. Distinct roles of dopamine D2L and D2S receptor isoforms in the regulation of protein phosphorylation at presynaptic and postsynaptic sites. Proc Natl Acad Sci USA 2003;100:4305–9.
[9] Montmayeur JP, Guiramand J, Borrelli E. Preferential coupling between dopamine D2 receptors and G-proteins. Mol Endocrinol 1993;7:161–70.
[10] Senogles SE. The D2 dopamine receptor isoforms signal through distinct Gi alpha proteins to inhibit adenylyl cyclase. A study with site-directed mutant Gi alpha proteins. J Biol Chem 1994;269:23120–7.
[11] Guiramand J, Montmayeur JP, Ceraline J, Bhatia M, Borrelli E. Alternative splicing of the dopamine D2 receptor directs specificity of coupling to G-proteins. J Biol Chem 1995;270:7354–8.
[12] Xu R, Hranilovic D, Fetsko LA, Bucan M, Wang Y. Dopamine D2S and D2L receptors may differentially contribute to the actions of antipsychotic and psychotic agents in mice. Mol Psychiatry 2002;7:1075–82.
[13] Seeman P, Chau-Wong M, Tedesco J, Wong K. Brain receptors for antipsychotic drugs and dopamine: direct binding assays. Proc Natl Acad Sci USA 1975;72:4376–80.
[14] Creese I, Burt DR, Snyder SH. Dopamine receptor binding predicts clinical and pharmacological potencies of antischizophrenic drugs. Science 1976;192:481–3.
[15] Deutch AY. Prefrontal cortical dopamine systems and the elaboration of functional corticostriatal circuits: implications for schizophrenia and Parkinson's disease. J Neural Transm Gen Sect 1993;91:197–221.
[16] Kapur S, Seeman P. Does fast dissociation from the dopamine d(2) receptor explain the action of atypical antipsychotics?: A new hypothesis. Am J Pychiatry 2001;158:360–9.
[17] Swinney DC. Biochemical mechanisms of drug action: what does it take for success? Nat Rev Drug Discov 2004;3:801–8.
[18] Swinney DC. Can binding kinetics translate to a clinically differentiated drug? From theory to practice. Lett Drug Des Discov 2006;3:569–74.

[19] Copeland RA, Pompliano DL, Meek TD. Drug-target residence time and its implications for lead optimization. Nat Rev Drug Discov 2006;5:730–9.
[20] Oliveira CR, Lima MC, Carvalho CA, Leysen JE, Carvalho AP. Partition coefficients of dopamine antagonists in brain membranes and liposomes. Biochem Pharmacol 1989;38:2113–20.
[21] Makriyannis A, Tian X, Guo J. How lipophilic cannabinergic ligands reach their receptor sites. Prostaglandins Other Lipid Mediat 2005;77:210–8.
[22] Niznik HB, Grigoriadis DE, Pri-Bar I, Buchman O, Seeman P. Dopamine D2 receptors selectively labelled by a benzamide neuroleptic: [3H]-YM-09151-2. Naunyn Schmiedebergs Arch Pharmacol 1985;329:333–43.
[23] Terai M, Hidaka K, Nakamura Y. Comparison of [3H]YM-09151-2 with [3H]spiperone and [3H]raclopride for dopamine d-2 receptor binding to rat striatum. Eur J Pharmacol 1989;173:177–82.
[24] Seeman P, Guan HC, Civelli O, Van Tol HH, Sunahara RK, Niznik HB. The cloned dopamine D2 receptor reveals different densities for dopamine receptor antagonist ligands. Implications for human brain positron emission tomography. Eur J Pharmacol 1992;227:139–46.
[25] Ng GY, O'Dowd BF, Lee SP, Chung HT, Brann MR, Seeman P, et al. Dopamine D2 receptor dimers and receptor-blocking peptides. Biochem Biophys Res Commun 1996;227:200–4.
[26] Vile JM, D'Souza UM, Strange PG. [3H]nemonapride and [3H]spiperone label equivalent numbers of D2 and D3 dopamine receptors in a range of tissues and under different conditions. J Neurochem 1995;64:940–3.
[27] Malmberg A, Jerning E, Mohell N. Critical reevaluation of spiperone and benzamide binding to dopamine D2 receptors: evidence for identical binding sites. Eur J Pharmacol 1996;303:123–8.
[28] Hall H, Wedel I, Halldin C, Kopp J, Farde L. Comparison of the in vitro receptor binding properties of *N*-[3H]methylspiperone and [3H]raclopride to rat and human brain membranes. J Neurochem 1990;55: 2048–57.
[29] Hara M, Tozawa F, Itazaki K, Mihara S, Fujimoto M. Endothelin ET(B) receptors show different binding profiles in intact cells and cell membrane preparations. Eur J Pharmacol 1998;345:339–42.
[30] Fierens FL, Vanderheyden PM, Roggeman C, Vande Gucht P, De Backer JP, Vauquelin G. Distinct binding properties of the AT(1) receptor antagonist [(3)H]candesartan to intact cells and membrane preparations. Biochem Pharmacol 2002;63:1273–9.
[31] Verheijen I, Vanderheyden PM, De Backer JP, Bottari S, Vauquelin G. Antagonist interaction with endogenous AT(1) receptors in human cell lines. Biochem Pharmacol 2002;64:1207–14.
[32] Vauquelin G, Morsing P, Fierens FL, De Backer JP, Vanderheyden PM. A two-state receptor model for the interaction between angiotensin II type 1 receptors and non-peptide antagonists. Biochem Pharmacol 2001;61: 277–84.
[33] Itokawa M, Toru M, Ito K, Tsuga H, Kameyama K, Haga T, et al. Sequestration of the short and long isoforms of dopamine D2 receptors expressed in Chinese hamster ovary cells. Mol Pharmacol 1996;49:560–6.
[34] Norman JA, Drummond AH, Moser P. Inhibition of calcium-dependent regulator-stimulated phosphodiesterase activity by neuroleptic drugs is unrelated to their clinical efficacy. Mol Pharmacol 1979;16:1089–94.
[35] Martres MP, Bouthenet ML, Sales N, Sokoloff P, Schwartz JC. Widespread distribution of brain dopamine receptors evidenced with [125I]iodosulpride, a highly selective ligand. Science 1985;228:752–5.
[36] Kim KM, Valenzano KJ, Robinson SR, Yao WD, Barak LS, Caron MG. Differential regulation of the dopamine D2 and D3 receptors by G protein-coupled kinases and beta-arrestins. J Biol Chem 2001;276:409–14.
[37] Armstrong D, Strange PG. Dopamine D2 receptor dimer formation: evidence from ligand binding. J Biol Chem 2001;276:22621–9.
[38] Vivo M, Lin H, Strange PG. Investigation of cooperativity in the binding of ligands to the D(2) dopamine receptor. Mol Pharmacol 2006;69:226–35.
[39] Dewar KM, Montreuil B, Grondin L, Reader TA. Dopamine D2 receptors labelled with [3H]raclopride in rat and rabbit brains. Equilibrium binding, kinetics, distribution and selectivity. J Pharmacol Exp Ther 1989;250:696–706.
[40] Lepiku M, Rinken A, Järv J, Fuxe K. Kinetic evidence for isomerization of the dopamine receptor–raclopride complex. Neurochem Int 1996;28:591–5.
[41] de Chaffoy De Courcelles D. The serotonin-S2 receptor: a receptor-transducer coupling model to explain insurmountable antagonist effects. Drug Dev Res 1986;8:173–8.
[42] Kenakin T. Agonist-receptor efficacy. II. Agonist trafficking of receptor signals. Trends Pharmacol Sci 1995;16:232–8.
[43] Vauquelin G, Van Liefde I. G protein-coupled receptors: a count of 1001 conformations. Fundam Clin Pharmacol 2005;19:45–56.
[44] Chatterjee TK, Scott CE, Vazquez DM, Bhatnagar RK. Interaction of [3H]spiperone with rat striatal dopamine D-2 receptors: kinetic evidence for antagonist-induced formation of ternary complex. Mol Pharmacol 1988;33: 402–13.
[45] Vauquelin G, Szczuka A. Kinetic versus allosteric mechanisms to explain insurmountable antagonism and delayed ligand dissociation. Neurochem Int 2007;51:254–60.
[46] DeMeyts P, Bainco AR, Roth J. Site-site interactions among insulin receptors. Characterization of the negative cooperativity. J Biol Chem 1976;251:1877–88.
[47] Park LS, Friend DJ, Schmierer AE, Dower SK, Namen AE. Murine interleukin 7 (IL-7) receptor. Characterization on an IL-7-dependent cell line. J Exp Med 1990;171:1073–89.
[48] Limbird LE. Cell surface receptors: a short course on theory and methods. Norwell, MA: Kulwer Academic Publishers; 1996.
[49] Gill R, Verma C, Wallach B, Urso B, Pitts J, Wollmer A, et al. Modelling of the disulphide-swapped isomer of human insulin-like growth factor-1: implications for receptor binding. Protein Eng 1999;12:297–303.
[50] Christopoulos A. Allosteric binding sites on cell-surface receptors: novel targets for drug discovery. Nat Rev Drug Discov 2002;1:198–210.
[51] Christopoulos A, Kenakin T. G protein-coupled receptor allosterism and complexing. Pharmacol Rev 2002;54:323–74.
[52] Gopalakrishnan M, Forsten-Williams K, Nugent MA, Täuber UC. Effects of receptor clustering on ligand dissociation kinetics: theory and simulations. Biophys J 2005;89: 3686–700.
[53] Fierens F, Vanderheyden PM, De Backer JP, Vauquelin G. Binding of the antagonist [3H]candesartan to angiotensin II AT1 receptor-transfected [correction of tranfected] Chinese hamster ovary cells. Eur J Pharmacol 1999;367:413–22.
[54] Sutter A, Riopelle RJ, Harris-Warrick RM, Shooter EM. Nerve growth factor receptors. Characterization of two distinct classes of binding sites on chick embryo sensory ganglia cells. J Biol Chem 1979;254:5972–82.
[55] Berg HC, Purcell EM. Physics of chemoreception. Biophys J 1977;20:193–219.
[56] DeLisi C. The effect of cell size and receptor density on ligand–receptor reaction rate constants. Mol Immunol 1981;18:507–11.

[57] Shoup D, Szabo A. Role of diffusion in ligand binding to macromolecules and cell-bound receptors. Biophys J 1982;40:33–9.
[58] Goldstein B, Posner RG, Torney DC, Erickson J, Holowka D, Baird B. Competition between solution and cell surface receptors for ligand. Dissociation of hapten bound to surface antibody in the presence of solution antibody. Biophys J 1989;56:955–66.
[59] Axelrod D, Wang MD. Reduction-of-dimensionality kinetics at reaction-limited cell surface receptors. Biophys J 1994;66:588–600.
[60] Tian X, Guo J, Yao F, Yang DP, Makriyannis A. The conformation, location, and dynamic properties of the endocannabinoid ligand anandamide in a membrane bilayer. J Biol Chem 2005;280:29788–95.
[61] Zoumpoulakis P. Seeking the active site of the AT1 receptor for computational docking studies. Drug Des Rev 2005;2:537–45.
[62] Lynch DL, Reggio PH. Cannabinoid CB1 receptor recognition of endocannabinoids via the lipid bilayer: molecular dynamics simulations of CB1 transmembrane helix 6 and anandamide in a phospholipid bilayer. J Comput Aided Mol Des 2006;20:495–509.
[63] Goldstein B. Cell surface receptors: models for binding, aggregation and signal initiation. Part A. Ligand-receptor binding and cell surface receptor dynamics, http://www.samsi.info/200405/compbio/SAMSInotes032405.pdf, 2005
[64] Gazi L, Wurch T, Lopéz-Giménez JF, Pauwels PJ, Strange PG. Pharmacological analysis of a dopamine D(2short): G(alphao) fusion protein expressed in Sf9 cells. FEBS Lett 2003;545:155–60.
[65] Kapur S, Seeman P. Antipsychotic agents differ in how fast they come off the dopamine D2 receptors. Implications of atypical antipsychotic action. J Psychiatry Neurosci 2000;25:161–6.